BRIEF REPORT

Fatal Case of Deer Tick Virus Encephalitis

Norma P. Tavakoli, Ph.D., Heng Wang, M.A., Michelle Dupuis, B.Sc., Rene Hull, B.A., Gregory D. Ebel, Sc.D., Emily J. Gilmore, M.D., and Phyllis L. Faust, M.D., Ph.D.

SUMMARY

Deer tick virus is related to Powassan virus, a tickborne encephalitis virus. A 62-year-old man presented with a meningoencephalitis syndrome and eventually died. Analyses of tissue samples obtained during surgery and at autopsy revealed a widespread necrotizing meningoencephalitis. Nucleic acid was extracted from formalin-fixed tissue, and the presence of deer tick virus was verified on a flavivirus-specific polymerase-chain-reaction (PCR) assay, followed by sequence confirmation. Immunohistochemical analysis with antisera specific for deer tick virus identified numerous immunoreactive neurons, with prominent involvement of large neurons in the brain stem, cerebellum, basal ganglia, thalamus, and spinal cord. This case demonstrates that deer tick virus can be a cause of fatal encephalitis.

From the Wadsworth Center, New York State Department of Health (N.P.T., H.W., M.D., R.H.), and the Department of Biomedical Sciences, School of Public Health, University at Albany (N.P.T.) — both in Albany; the Department of Pathology, University of New Mexico School of Medicine, Albuquerque (G.D.E.); and the Departments of Neurology (E.J.G.) and Pathology and Cell Biology (P.L.F.), Columbia University, and New York Presbyterian Hospital (E.J.G., P.L.F.) — both in New York. Address reprint requests to Dr. Tavakoli at the Empire State Plaza, P.O. Box 509, Albany, NY 12201, or at norma.tavakoli@wadsworth.org.

N Engl J Med 2009;360:2099-107.

DEER TICK VIRUS IS A MEMBER OF THE TICKBORNE ENCEPHALITIS GROUP of flaviviruses and is closely related to Powassan virus. Deer tick virus was first isolated from *Ixodes scapularis* ticks in 1997 in North America.[1] The complete sequence of the deer tick virus has been determined.[2] The viral genome is 10.8 kb in length and shares 84% nucleotide sequence identity and 94% amino acid sequence identity with the Powassan virus genome. The two viruses are antigenically related,[3] and it has been suggested that they share a common origin and represent two viral lineages related to Powassan virus in North America.[2] Ebel et al.[4] refer to deer tick virus as Powassan virus lineage II, and in this report we use the same terminology.

Several members of the tickborne encephalitis group of flaviviruses, including tickborne encephalitis virus and Powassan virus, cause encephalitis in humans and animals, with tickborne encephalitis virus causing the most serious outbreaks. These viruses are closely related antigenically and are found predominantly in the northern hemisphere. In Europe, tickborne encephalitis occurs mainly in eastern and central regions and affects approximately 50 to 199 persons per 100,000 inhabitants annually.[5] The seroprevalence of antibodies to Powassan virus is estimated to be 0.5 to 4.0% in areas in which the disease is endemic.[6]

Infection with tickborne encephalitis virus can be mild or asymptomatic, or it can result in meningitis and encephalitis. Powassan virus can be pathogenic in human beings and can cause severe encephalitis with a fatality rate of up to 60% and long-term neurologic sequelae in survivors.[7] In contrast, Central European encephalitis that is caused by tick bites typically produces mild or silent infection. Other disease-causing flaviviruses include West Nile virus, St. Louis encephalitis virus, dengue virus, and yellow fever virus.[8] These viruses are transmitted by mosquitoes and cause a spectrum of diseases including meningitis, encephalitis, dengue fever, and yellow fever.

In certain locations of the northeastern and north central United States, the prevalence of deer tick virus in adult deer ticks is high,[9,10] but human infection has not been reported previously. This could indicate that the virus does not easily infect humans or that it is not particularly pathogenic. Diagnostic testing for Powassan virus is not routinely performed for patients with symptoms of encephalitis. Human incidence may thus be currently underestimated.

CASE REPORT

In late spring, a 62-year-old man was admitted to a local New York State hospital with a 4-day history of fatigue, fever, bilateral maculopapular palmar rash, and an onset of diplopia, dysarthria, and weakness in the right arm and leg. He was a native of New York State and had no history of recent travel. He owned horses and spent time outdoors in a wooded area. Reports of Lyme disease were common in his county of residence, indicating tick activity in the area. His medical history included chronic lymphocytic leukemia–small lymphocytic lymphoma (CLL–SLL), which had been diagnosed 4 years earlier and had initially been treated with fludarabine. He was not taking corticosteroids. On admission, he was given nonsteroidal antiinflammatory medication and an oral antibiotic (amoxicillin–clavulanate), which had been prescribed by his primary care physician for a recent exacerbation of chronic sinusitis that had been recurrent for more than a year. His baseline white-cell count was 15,000 cells per cubic millimeter and had increased to 70,000 cells per cubic millimeter during the past 6 to 8 months. He was started on broad-spectrum antibiotics and acyclovir (700 mg administered intravenously every 8 hours) for presumed infection of the central nervous system. The differential diagnosis included cerebral ischemia, possibly related to leukostasis, infection (viral, bacterial, or fungal), and lymphoma.

Initial laboratory results were notable for a markedly elevated peripheral-blood white-cell count (144,200 cells per cubic millimeter) and cerebrospinal fluid with normal glucose, minimally elevated protein, no white cells, and a negative Gram's stain (Table 1). The erythrocyte sedimentation rate was 4, blood cultures were sterile, and antibody titers were negative for *Borrelia burgdorferi* and *Anaplasma phagocytophilum*. The neurologic symptoms progressed, and after 2 days he was transferred to another hospital. At the time of transfer, the peripheral-blood white-cell count was 174,800 per cubic millimeter (with 4% neutrophils and 94% lymphocytes) (Table 1).

Findings on flow cytometry were characteristic of CLL–SLL. Bacterial and fungal blood cultures were sterile. Sputum cultures for tuberculosis and legionella species were negative. No serum antibodies to *Bartonella henselae* or leptospira or brucella species were detected. One day after admission, a repeat spinal tap showed an elevated protein level of 192 mg per deciliter, lymphocytic pleocytosis with 891 cells per cubic millimeter (with 1% neutrophils and 93% lymphocytes), and a normal glucose level (Table 1). Flow cytometry of the cerebrospinal fluid demonstrated a predominantly reactive T-cell population (98% of CD45+ cells were CD3+/CD5+ small T cells), with no evidence of CLL–SLL. Bacterial culture and Gram's staining of the cerebrospinal fluid were negative. India-ink staining, cryptococcus antigen test, and PCR analyses for herpes simplex virus types 1 and 2 and JC–BK virus were negative in cerebrospinal fluid.

Magnetic resonance imaging (MRI) performed after transfer (hospital day 1) revealed abnormal T_2-weighted and fluid-attenuated inversion recovery (FLAIR) images, with hyperintensities most prominent in the superior cerebellum, left pons, and bilateral basal ganglia (Fig. 1A, 1B, and 1C). An axial diffusion-weighted image and apparent-diffusion-coefficient sequences revealed restricted diffusion in the superior cerebellum, suggesting an ischemic process (Fig. 1D). The patient remained febrile (maximum temperature, 104.5°F [40.3°C]), and antimicrobial coverage was broadened to include an antifungal agent. His neurologic function deteriorated, which necessitated intubation, and his function did not improve despite maximal medical therapy.

On hospital day 4, his fever abated, and computed tomographic imaging revealed a mild obstructive hydrocephalus, leading to placement of an external ventricular drain. On hospital day 5, repeat MRI revealed worsening of signal abnormalities and markedly increased hydrocephalus. He was taken urgently to the operating room for decompression with a suboccipital craniotomy, at which time cerebellar biopsy was performed. Analysis of the biopsy specimen revealed severe meningoencephalitis with a dense meningeal lymphoid infiltrate containing mainly reactive CD4+ T cells, lymphocytic venous invasion and destruc-

tion, widespread loss of cerebellar Purkinje cells, occasional microglial nodules, and marked Bergmann gliosis (Fig. 1A to 1H in the Supplementary Appendix, available with the full text of this article at NEJM.org). The parenchyma was infiltrated by activated microglia–macrophages and predominantly CD8+ T cells (Fig. 1I and 1J in the Supplementary Appendix). All biopsy cultures were negative, and staining of biopsy tissue was negative for bacterial, fungal, and mycobacterial organisms and viral antigens (including herpes simplex virus 1 and 2, varicella–zoster virus, cytomegalovirus, influenza A, parainfluenza 3, adenovirus, and parvovirus).

MRI of the brain on hospital day 7 revealed progression of signal abnormalities, new lesions in the right thalamus and bilateral cerebral hemispheres, and persistent hydrocephalus (Fig. 2 in the Supplementary Appendix). By hospital day 11, there was no improvement in his status. Life support was withdrawn, and he died 17 days after the onset of symptoms. An autopsy was performed.

METHODS

CLINICAL SPECIMENS

A surgical biopsy of the cerebellum was fixed in formalin and embedded in paraffin. After autopsy, the brain was formalin-fixed for 2 weeks, and standard tissue blocks were paraffin-embedded. Unembedded, formalin-fixed brain tissue from the midbrain, cerebellum, pons, and spinal cord was submitted for PCR testing. (For details on viruses and control samples that were used, see the Methods section in the Supplementary Appendix.)

REVERSE-TRANSCRIPTASE–PCR AND SEQUENCE ANALYSIS

Nucleic acid was extracted from formalin-fixed tissue with the use of the WaxFree DNA extraction kit (TrimGen). This kit coextracts RNA. Ten microliters of extracted nucleic acid was reverse-transcribed to complementary DNA (cDNA) with the use of the iScript cDNA synthesis kit (Bio-Rad). Heminested reverse-transcriptase PCR (RT-PCR) for the detection of flavivirus with the use of universal primers was performed as described previously.[11,12] (In the Supplementary Appendix, additional information on the PCR primers is listed in Table A, and details regarding the PCR methods, sequence, and histologic and immunohistochemical analyses are listed in the Methods section.)

Table 1. Results of Analysis of Cerebrospinal Fluid and Blood of the Patient.*

Variable	First Hospitalization	Day 1 after Transfer to Second Hospital	Normal Range
Cerebrospinal fluid			
Glucose level (mg/dl)	59	47	40–70
Protein level (mg/dl)	64	192	15–45
White-cell count (cells/mm^3)	0	891	0–5
Neutrophils (%)		1	0
Lymphocytes (%)		93	70
Complete blood count			
White-cell count (cells/mm^3)	144,200	174,800	3500–9100
Neutrophils (%)	2	4	38–80
Lymphocytes (%)	98	94	15–40

* To convert the values for glucose to millimoles per liter, multiply by 0.05551.

RESULTS

The general autopsy revealed diffuse lymphadenopathy and splenomegaly and infiltration of liver and kidney by CLL–SLL. The brain weight was 1810 g (normal range in adults, 1300 to 1350), consistent with marked edema. On sectioning, there was marked softening and grayish discoloration throughout the brain stem and cerebellum.

Histologic examination of the brain revealed widespread meningopolioencephalitis and meningopoliomyelitis; there was no evidence of infiltration by CLL–SLL. A mild meningeal lymphocytic infiltrate persisted, and dense perivascular infiltrates were still identified in the parenchyma (Fig. 3C to 3K in the Supplementary Appendix). Throughout the brain, multinodular to patchy mononuclear infiltrates and confluent areas of necrosis were identified, along with microglial nodules and neuronophagia. This was most accentuated in large motor neurons of the brain stem (including cranial nerve nuclei), spinal anterior horns, cerebellum, basal ganglia, and thalamus (Fig. 2, and Fig. 3 in the Supplementary Appendix). Microglia–macrophage infiltration was greatest in gray-matter regions but also involved white-matter tracts to a lesser degree (Fig. 3A in the Supplementary Appendix).

As in the surgical biopsy, lymphocytic infiltrates in leptomeninges and perivascular spaces contained predominantly CD4+ helper T cells, whereas those in the parenchyma were predominantly CD8+ cytotoxic T cells (Fig. 4 in the Supplementary Appendix). CD8+ T cells were also

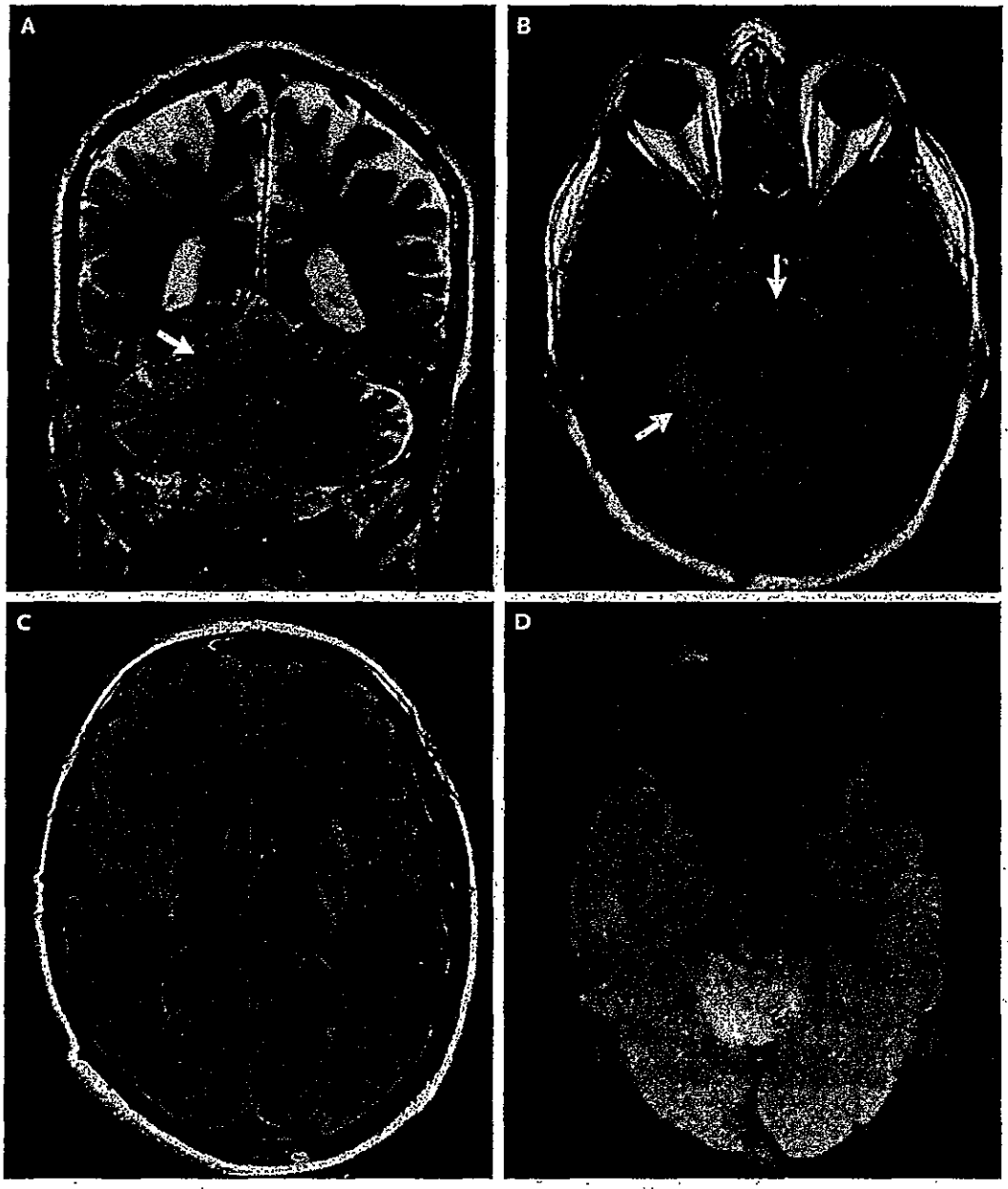

Figure 1. Magnetic Resonance Imaging (MRI) of the Brain on Hospital Admission.

MRI scanning that was performed on hospital day 1 revealed abnormal T_2-weighted signaling in the superior cerebellum (Panel A, arrow) and abnormal T_2-weighted fluid-attenuated inversion recovery images with hyperintensities in the cerebellum and left pons (Panel B, arrows) and in the bilateral basal ganglia (Panel C). The superior cerebellum was bright on diffusion-weighted imaging (Panel D) and dark on apparent-diffusion-coefficient sequences, which suggested an ischemic process.

more frequently identified in close apposition to surviving neurons (Fig. 2C, and Fig. 4A, 4B, and 4E in the Supplementary Appendix).

On the extracted nucleic acid from the formalin-fixed brain tissue, the following analyses were performed: a PCR panel including real-time PCR assays for the detection of herpes simplex viruses 1 and 2, Epstein–Barr virus, cytomegalovirus, human herpesvirus type 6, varicella–zoster virus, and adenovirus; real-time RT-PCR assays for the de-

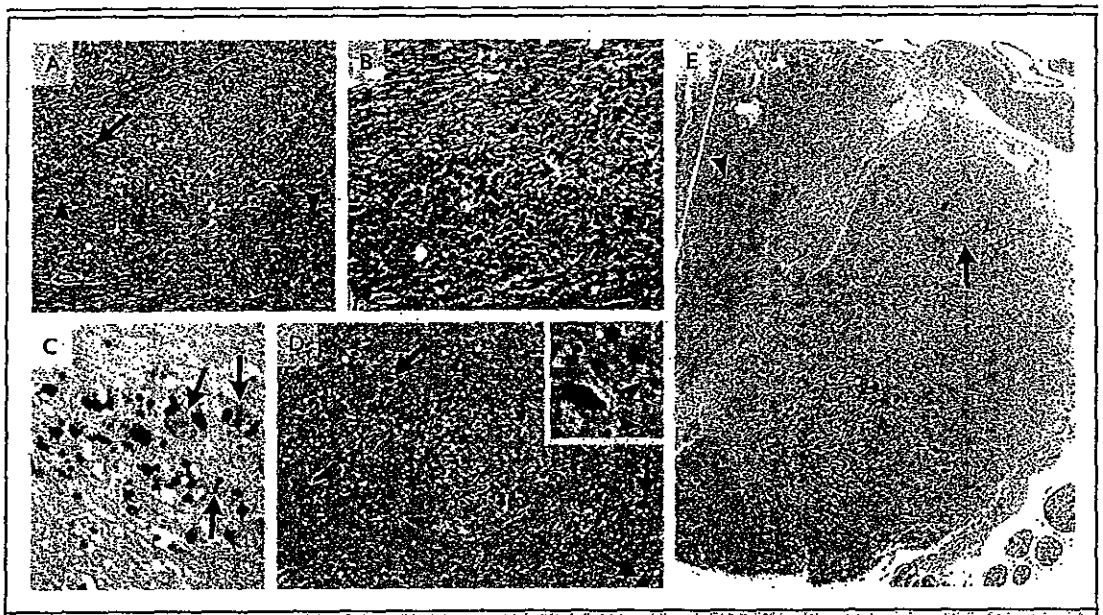

Figure 2. Histologic Findings at Autopsy.

In Panel A, microglial nodules and lymphocytic infiltrates in the pons are visible in basal pontine nuclei (arrowheads), with less prominent involvement of descending fiber tracts (arrow) and pontocerebellar fibers. In Panel B, confluent foci of parenchymal necrosis can be seen in pontine basal nuclei. In Panel C, CD8+ immunostaining of the basis pontis shows a cytotoxic T-cell infiltrate and a close association with surviving neurons (arrows). In Panel D, nearly complete neuronal loss is seen in the substantia nigra with rare surviving neurons (arrows); in the inset, an eosinophilic dying neuron and remaining neuromelanin pigment are engulfed in macrophages or free in the parenchyma (arrowheads). In Panel E, phosphoglucomutase 1 immunostaining of lumbar spinal cord shows marked infiltration by microglia–macrophages and in the anterior horn and focal microglial nodules in the lateral corticospinal tract (arrow) and posterior column (arrowhead). In Panels A, B, and D, paraffin sections were stained with hematoxylin and eosin.

tection of West Nile virus and eastern equine encephalitis virus; a real-time PCR assay using a cDNA template for the detection of enterovirus; a group-specific RT-PCR assay for the detection of alphaviruses[13]; and conventional PCR assays using a cDNA template for the detection of St. Louis encephalitis, California serogroup, and Cache Valley viruses. PCR assays for the detection of borrelia species, including *B. burgdorferi*, and of *A. phagocytophilum* were performed on DNA extracts from the cerebellum and spinal cord. All results were negative. A group-specific RT-PCR assay for the detection of flaviviruses gave PCR products of the expected size for both the first-round PCR and the nested PCR.[11] The PCR products of approximately 250 bp and 220 bp were purified from the gel and sequenced. A search with the use of the nucleotide Basic Local Alignment Search Tool (BLAST) algorithm posted on the Web site of the National Center for Biotechnology Information identified a 220-bp sequence sharing 97% of the sequence of deer tick virus strains CTB30 (accession number, AF311056.1), and IPS001 (accession number, AF310947.1) and Powassan virus strain R59266 (accession number, AF310948.1). To confirm the lineage of the virus, sequencing was performed with the use of previously published and newly designed primer sets from the envelope coding region, NS5, and sequences in the 3′ untranslated region[3,4] (Table A in the Supplementary Appendix).

With a total of 23 primer sets used, two regions of the virus were sequenced: 2748 bp, spanning part of the RNA polymerase coding sequence and the 3′ untranslated region of the virus, and 1180 bp of the envelope coding sequence. Phylogenetic analyses of these fragments indicated that the virus, named DT-NY-07, was most closely related to the deer tick virus (Fig. 3).[14-16]

To confirm that deer tick virus antigens were detectable in brain tissue from the patient, two polyclonal mouse antibody reagents were generated against whole deer tick virus and recombinant deer tick virus E protein (rEDTV). Both antiserum samples showed similar immunohistochemical specificity in both the cerebellar biopsy and au-

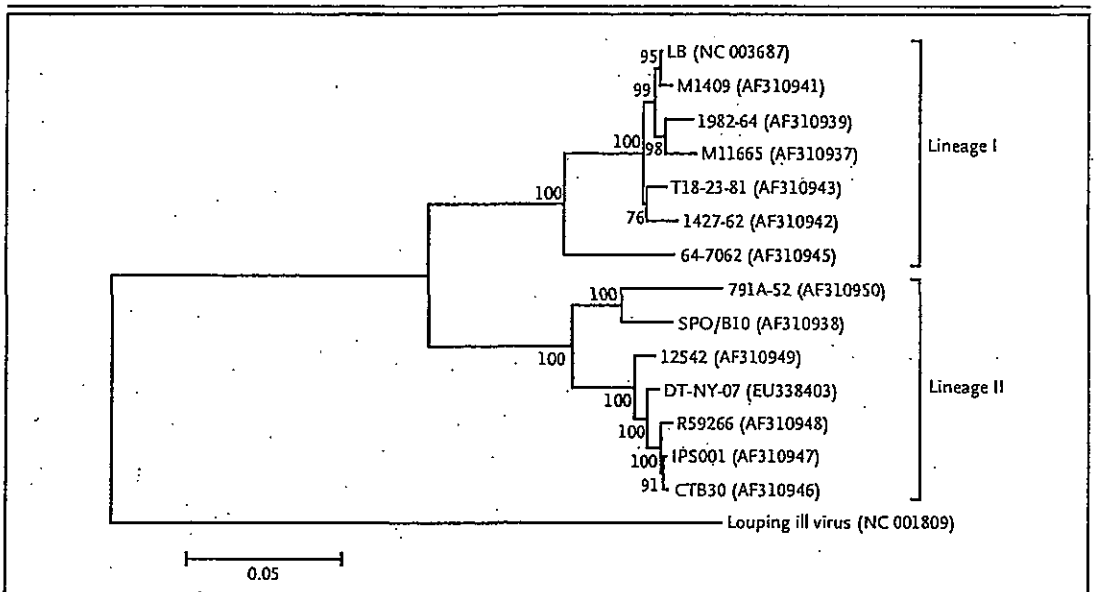

Figure 3. Phylogenetic Tree Showing the Relationship between the Virus (DT-NY-07) Detected in Tissue Sections from the Brain of the Patient and Other Powassan Viruses.

This phylogenetic tree was constructed from 2304 nucleotide sequences of the NS5 region. GenBank accession numbers are in parentheses. The evolutionary history was inferred with the use of the neighbor-joining method.[14] The optimal tree with the sum of branch length equaling 0.60849794 is shown. The percentage of replicate trees in which the associated taxa are clustered together in the bootstrap test (1000 replicates) is shown next to each branch. The tree is drawn to scale, with branch lengths in the same units as those of the evolutionary distances used to construct the phylogenetic tree. To root the dendrogram, louping ill virus was used as the outgroup. The evolutionary distances were computed with the use of the maximum-composite-likelihood method[15] and are expressed in the units of the number of base substitutions per site. All positions containing gaps and missing data were eliminated from the data set. Phylogenetic analyses were conducted with the use of Molecular Evolutionary Genetics Analysis (MEGA) software, version 4.0.[16]

topsy specimens, although generally a larger number of neurons and viral antigens in macrophages were labeled with the whole-virus serum (Fig. 4, and Fig. 5 in the Supplementary Appendix). The whole-virus antiserum labeled neuronal-cell bodies, dendrites, and axons. The rEDTV serum and rarely the whole-virus serum also labeled rounded, granular-to-tubular profiles within the neuronal cytoplasm of large motor neurons, with a cellular distribution highly reminiscent of the Golgi apparatus in some neurons (Fig. 4A, and Fig. 6 in the Supplementary Appendix). Alternatively, the structures may represent viral particles within the lysosomal–endosomal system. A segmental distribution of labeled neurons was prominent in the hippocampus (Fig. 4B). In isocortical regions, occasional labeled neurons and a focus of infected cells consistent with oligodendrocytes were also identified (Fig. 4D).

DISCUSSION

Strains of Powassan virus lineages I and II are distinct and are maintained in separate enzootic cycles because of differences in transmission vectors and geographic distribution. Lineage I strains are transmitted by ticks and have been reported in North America (mainly in New York State and Canada) and in eastern Russia, whereas lineage II strains have been isolated in the Atlantic Coast of the United States and in Wisconsin.[4] Lineage I strains appear to be associated with *I. cookei* and groundhogs (*Marmota monax*), whereas lineage II strains are associated with deer ticks and white-footed mice (*Peromyscus leucopus*).[7] In addition, lineage II strains have not previously been associated with human disease, whereas a number of infections in humans associated with lineage I strains have been documented.[17-21] From these re-

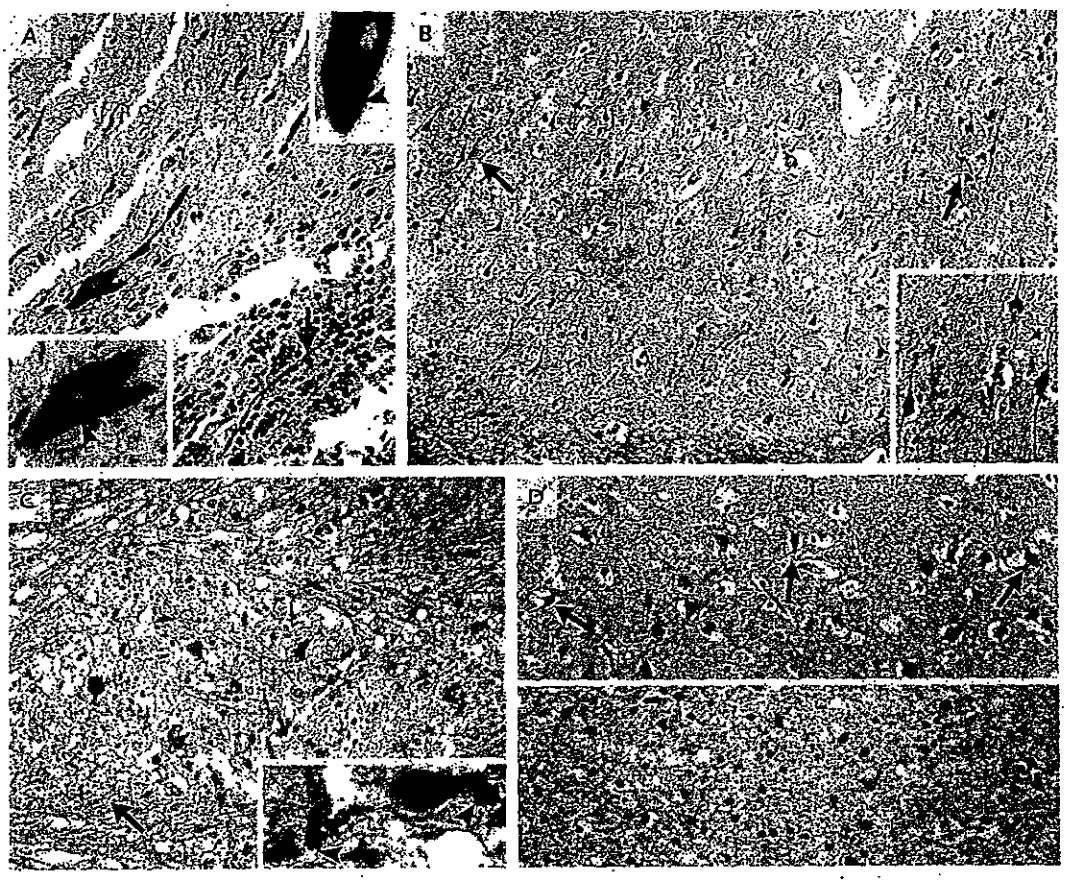

Figure 4. Immunohistochemical Analysis with Deer Tick Virus Antiserum Samples.

Paraffin sections of cerebellar samples obtained from the patient on biopsy (Panel A) and samples from the hippocampus (Panel B), pons (Panel C), and temporal cortex (Panel D) obtained at autopsy were stained either with antibody against whole deer tick virus (Panel A, upper inset, and Panels B and C) or with antibody against recombinant deer tick virus E protein (rEDTV) (Panel A, Panel A, lower inset, and Panel D). In Panel A, in the cerebellar-biopsy sample, both types of antiserum recognized surviving Purkinje cells, with prominent filling of their dendrites in the molecular layer and occasional identification of axons in the granule-cell layer (arrow); in the insets, several Purkinje cells were identified with immunoreactive granular-to-tubular profiles (arrowheads). In Panel B, many hippocampal pyramidal neurons were immunolabeled in a segmental distribution (in area surrounding arrows), with prominent decoration of apical and basal processes (inset). In Panel C, many surviving immunolabeled neurons in the basis pontis are visible. The whole deer tick virus antibody also recognized viral antigens engulfed in macrophages (arrow; inset, arrowheads), whereas the rEDTV antibody did not have such recognition. In Panel D, in temporal cortex, immunoreactive neurons that were not associated with inflammatory reaction were occasionally identified (upper panel, arrows). In the temporal white matter, a focus of labeled cells consistent with oligodendrocytes was seen (lower panel). (For more details, see Fig. 5 and 6 in the Supplementary Appendix.)

ports, it appears that lineage I Powassan encephalitis is characterized by respiratory distress, fever, vomiting, convulsions, and occasionally paralysis.[17,19] Studies in the northern Ontario region of Canada show an antibody prevalence rate of as much as 3.2%, indicating that infection does not always cause severe disease.[22] In a phylogenetic study of Powassan-related viruses of North America, a lineage II strain (ON97) was reportedly isolated from human brain tissue.[2] However, no other information regarding the case was provided.

Confirmation of infection with a lineage I strain of Powassan virus has been made principally by serologic methods. Because of serologic